

A Review on Recent Advancements in Rare-Earth based Double Perovskite Compounds

Charu Agarwal¹, Hitesh Mittal¹, Tabassum Bano¹, Jitendra Kumar¹, Mahendra Gora¹, Arvind Kumar¹, Subhash Chandra¹, Sagar Vikal², Yogendra K. Gautam², Sanjay Kumar^{1*}

¹Department of Physics, University of Rajasthan, Rajasthan 302004, India

²Department of Physics, Ch. Charan Singh University Meerut, Meerut, U.P.250004, India

Review Article

Received: 23-March-2022

Manuscript No. JPAP-22-58269-;

Editor assigned: 25- March-2022

Pre QC No. JPAP-22-58269(PQ);

Reviewed: 08-April-2022, QC No.

JPAP-22-58269; **Revised:** 12-April-

2022, Manuscript No. JPAP-22-

58269(A) **Published:** 15-April-2022,

DOI:10.4172/2320-2459.10.3.004

***For Correspondence:**

Sanjay Kumar, Department of Physics, University of Rajasthan, Rajasthan 302004, India

E-mail:

charuagarwal2310@gmail.com

Keywords: Perovskite compounds ; Dielectrics; Metal elements ; photo detector

ABSTRACT

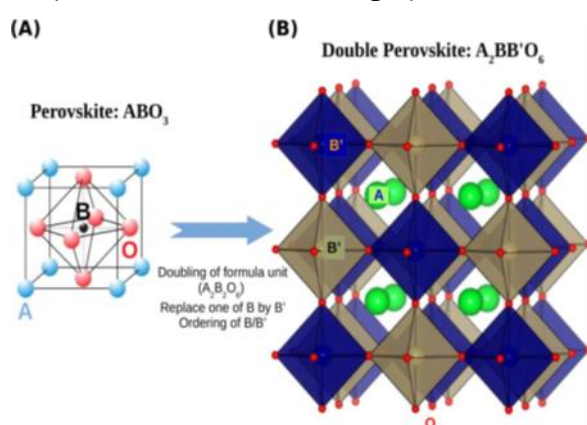
Double Perovskites (DP) materials with the rare-earth based compound is the most and widely studied due to its various fascinating properties such as magnetic, structural, electrical and optical properties. In this article, we comprehensive reviewed the structural as well as magnetic properties of A_2XMnO_6 (A=La, Nd and X=Cr, Ni, V) double perovskite compounds. It has been found that the Rare-Earth Based Double Perovskite (REBDP) compounds exhibits different structural and magnetic properties by changing the synthesis methods. Moreover, magnetic field and temperature affect the electronic and magneto electric characteristic of REBDP. These changes occur because of different exchange interactions such as super exchange interaction and double exchange interaction. Therefore, this review helps to exaggerate the new properties of these materials by introducing another synthesis method. In addition, a wide window is open where the ions at A site and X site can be varied to explore the new materials which are environment friendly and energy efficient

INTRODUCTION

At present, double perovskite compounds bring so much attention because of their fascinating properties [1-4]. Perovskite materials are skillfully investigated for a considerable range of gripping properties. It is well known that

single perovskite materials are very flexible in their structural and compositional property [5]. To extend the properties of perovskite material, the standard way is to substitute the cation place by other cations. Figure 1 predicts that if we merge two units of perovskites, then we obtain $A_2B_2O_6$ type double perovskites compounds in which half of B site ions is replaced by B'. Due to this substitution and arrangement between B and B' with corner-sharing BO_6 and $B'O_6$ octahedral units double perovskite structure $A_2BB'O_6$ is acquired. A site cation occupies every hole created by BO_6 and $B'O_6$ octahedra, as demonstrated in Figure 1. In $A_2BB'O_6$ structure B and B' are transition metal elements and A is alkaline material. Cation at A site is 12-fold oxygen coordinated while B and B' cations are 6-fold oxygen coordinated [6]. When Double Perovskite compounds, electronic properties dominantly affected by cations at B-site. It is not surprising that the variety of properties like metallic, half-metallic, semiconducting, dielectrics, thermoelectric, ferroelectric and superconducting are found in La_2NiFeO_6 , Sr_2CoIrO_6 and Sr_2FeMoO_6 compounds [7-9].

Figure 1. Structure of double perovskite material from single perovskite unit material.



Some of $A_2BB'O_6$ have been studied to show metal-insulator transition, such as Sr_2CoTiO_6 has a transition temperature of about 700 K [10]. Half-metallic properties of double perovskite materials are useful in spintronic devices. Some $A_2BB'O_6$ compounds show magneto resistance behavior, even though they were not half-metallic such as La_2CoMnO_6 [11,12]. Since most of the $A_2BB'O_6$ perovskites are insulators that can be studied to enhance the properties for microwave applications. Few layered $A_2BB'O_6$ perovskites such as $Sr_2Y(Ru_{1-x}Cu_x)O_6$ with high Curie temperature (T_c), shows superconductivity [13]. Low thermal conductivity reported in Sr_2CoReO_6 which results thermoelectric and photo catalytic properties in the material [14,15]. These materials show a variety of magnetic properties by introducing paramagnetic cations at all three sites. Magnetic characteristics rely on the spatial orbital overlap of different cations. $A_2BB'O_6$ compounds show different magnetic properties such as Anti Ferro Magnetic (AFM) [16], Ferro Magnetic (FM) [17], spin-glass behavior [18] and ferrimagnetism [19]. In $A_2BB'O_6$, B and B' forms Face Centered Cubic (FCC) lattices, which are responsible for AFM in these materials [20]. $A_2BB'O_6$ such as $R_2B'MnO_6$ where $B'=Co, Ni$ and R stands for rare earth ions shows ferromagnetic super exchange interaction between two B-site cations that are highly ordered structurally distorted [21-23]. Sr_2NiUO_6 shows ferromagnetic nature in which cause of magnetic ordering is not only super exchange interactions but also the moving electrons. Double perovskite showing ferrimagnetism can further splits into two groups; first for which $T_c > 300$ K are mainly metallic or half metallic and second for which $T_c < 200$ K are generally insulating. Spin flop or meta-magnetic transitions are also found in Sr_2NiReO_6 , Nd_2LiRuO_6 and Sr_2YIrO_6 . Reason of this transition is spin reorientation caused by an external magnetic field.

LITERATURE REVIEW

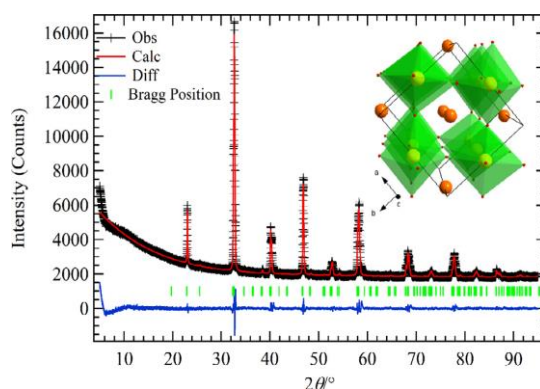
Recent studies demonstrated that these compounds show multi ferocity, such as in $\text{Pb}_2\text{FeTiO}_6$ [24]. The synchronicity of ferroelectric and ferromagnetic behavior at room temperature makes these materials applicable for spintronic devices. Some $\text{A}_2\text{BB}'\text{O}_6$ perovskite such as $\text{Ba}_2\text{PrBiO}_6$ are found as electrode materials which are used in solid oxide fuel cells [25]. Halide-based double perovskite material can be used for optoelectronic applications like X-ray detector, photo detector, light-emitting diode, photocatalyst and solar cell [26]. Since the last few decades, much research has been dedicated to double perovskite material [27,28]. In this review article, we have mainly discussed $\text{A}_2\text{BB}'\text{O}_6$ type double perovskite materials where A site ions can be rare-earth element (La, Nd, Sr) and B and B' site ions can be transition metal element (Cr, Ni, Mn, V). Our main aim is to exaggerate the engrossing magnetic properties and structural properties of these materials. Its electronic arrangement vacillating from insulating to metallic and half-metallic and magnetic ordering range vary from anti-ferromagnetic to ferromagnetic within a single material as we change the synthesis process of the material [27,33]. Above all, the thorough literature survey so far allows us to predict new environment friendly $\text{A}_2\text{BB}'\text{O}_6$ compounds yet to be synthesized and to find the correlation between electrical, magnetic, optical and structural characteristics.

Schematic of $\text{La}_2\text{CrMnO}_6$

Double Perovskite material La_2XMnO_6 (X=Cr) show magneto dielectric, magneto capacitance, and magneto resistance properties, making them suitable for magneto electric devices [34]. Literature review suggests that $\text{La}_2\text{CrMnO}_6$ (LCMO) differs remarkably in the electrical and magnetic properties using different synthesis conditions. These differences arise due to change in crystal structures, which are related to the electrical and magnetic properties. Hence, synthesis condition directly affects electrical and magnetic properties [35-37]. The previous report predicted that synthesis of LCMO material by ceramic technique had a monoclinic phase and deformation from ideal cubic symmetry [38]. While LCMO synthesized by combustion method, show rhombohedra structure with space group R3c. Then, Palalkal, et al. used the combustion method to synthesize LCMO, where citric acid was used as fuel. The observed structure was orthorhombic with space group Pbnm. Thus, in general researchers reported the structure of $\text{La}_2\text{CrMnO}_6$ which was orthorhombic with space group Pbnm.

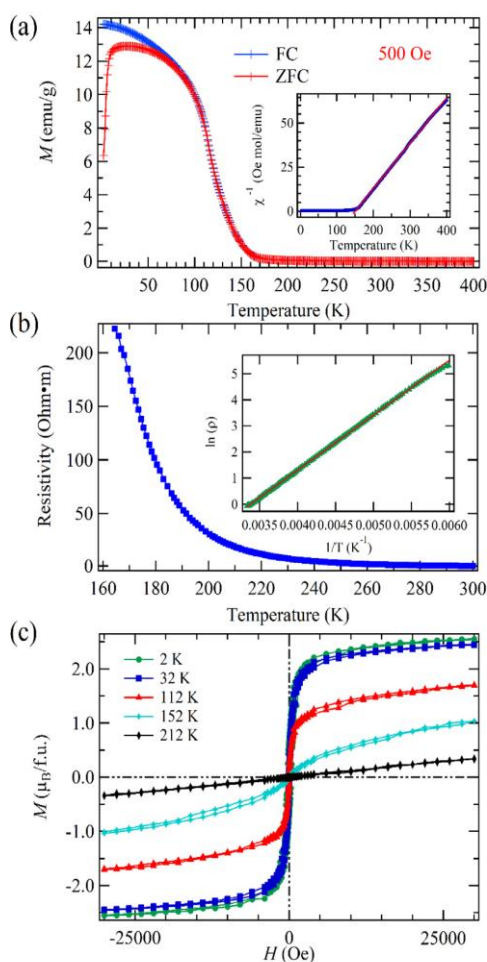
Magnetic exchange interactions have been studied extensively in LCMO. Sun et al. and Borrozo et al. acquired that the magnetism in LCMO is originated because of double exchange interaction of $\text{Cr}^{+3}\text{-O}^{2-}\text{-Cr}^{+3}$. Karpinsky et al. [39] reported that reason of ferromagnetic behavior in LCMO is $\text{Mn}^{+3}\text{-O}^{2-}\text{-Mn}^{+3}$ super exchange interaction and anti-ferromagnetic behavior is due to negative $\text{Cr}^{+3}\text{-O}^{2-}\text{-Cr}^{+3}$ interaction [40-45]. Yang synthesized LCMO by solid-state reaction method with precursors as La_2O_3 , MnO_2 ; Cr_2O_3 mixed them in ethanol for 6h and dried it for 12 h at 353 K.

Figure 2. XRD result of $\text{La}_2\text{CrMnO}_6$. Note: (—) Obs; (—) calc; (—) Diff; (|) Bragg Position



Structural results of solid state synthesized LCMO [46] as shown in Figure 2 reveal that the crystal structure of LCMO is orthorhombic with space group Pbnm and lattice parameters are $a=5.5224(2)\text{\AA}$, $b=5.4800(2)\text{\AA}$, $c=7.7680\text{\AA}$. Magnetic nature of LCMO sample prepared via solid state reaction [46] was done by Magnetic Property Measurement System (MPMS). ZFC and FC magnitudes were accomplished in temperature extent 2 K to 400 K, Yang reported that material showed ferrimagnetic or ferromagnetic transition at a temperature ~ 118 K, as shown in Figure 3. Further, the magnetic hysteresis loop curve was traced out at various temperatures (2 K, 32 K, 112 K, 152 K, and 212 K) to confirm the actual magnetic behavior of the sample. Yang confirmed ferromagnetic behavior in LCMO.

Figure 3. A. FC and ZFC of $\text{La}_2\text{CrMnO}_6$ at 2 K–400 K. Inset is inverse susceptibility and temperature. Note: (—) FC; (---) ZFC ; B. Resistivity versus temperature curve without applying a magnetic field; C. Magnetization (M) versus applied magnetic field (H). Note: (—) 2 K; (—) 32 K; (—) 112 K; (—) 152 K; (—) 212 K



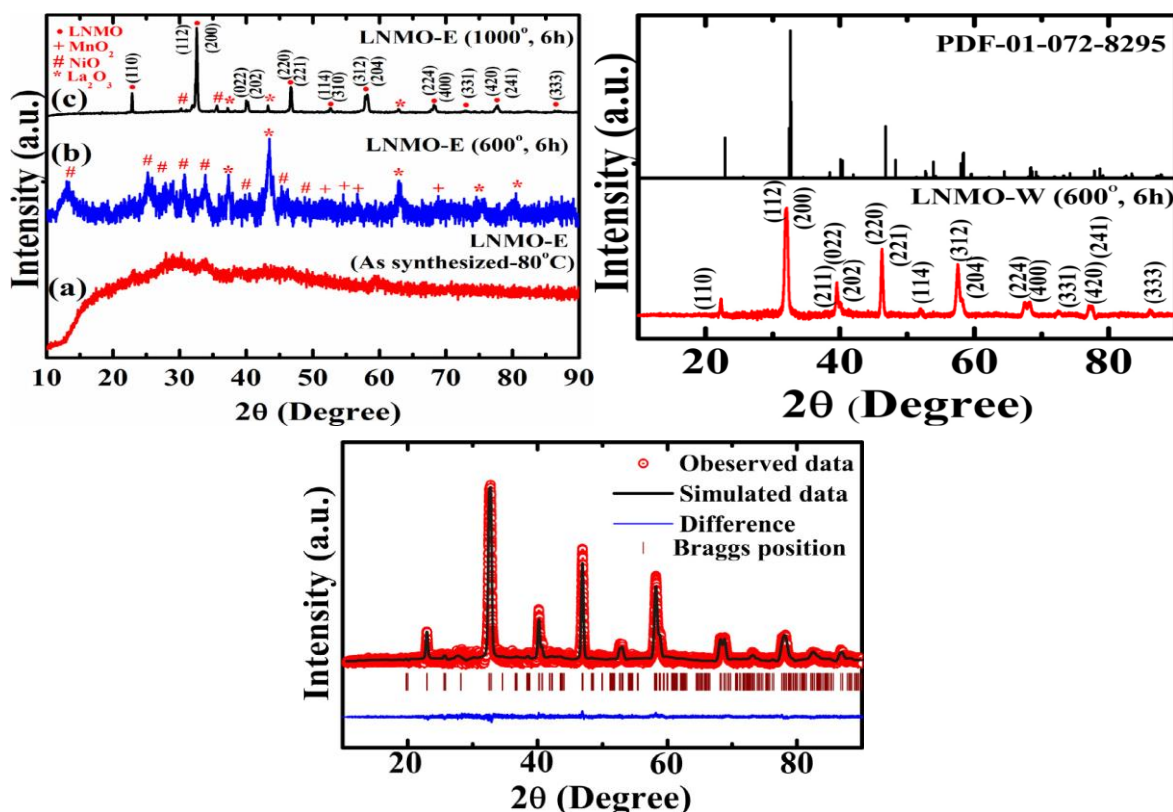
Schematic of $\text{La}_2\text{NiMnO}_6$

In double perovskites compounds, $\text{La}_2\text{NiMnO}_6$ (LNMO) is largely studied due to its unique and stable ferromagnetic insulating phase. Its Curie temperature (T_c) is nearly about room temperature. LNMO is widely used in many potential devices like sensor, memory device, radio frequency filter and phase shifter [47,48]. Due to various electronic interactions such as $\text{Ni}^{2+}\text{-O-Mn}^{4+}$ interactions, this compound is still open for researchers to design multipurpose functional materials. It is found that LNMO shows ferromagnetism through $\text{Mn}^{4+}\text{-O-Ni}^{2+}$ interchange interaction [49].

In contrast, Mn^{4+} -O- Mn^{4+} and Ni^{2+} -O- Ni^{2+} interchange interaction leads to antiferromagnetic in LNMO. So, these interactions affect the overall magnetic properties of LNMO [50]. LNMO was synthesized through solid-state reaction at temperature $\geq 723^\circ C$, found coexistence of monoclinic phase ($P2_1/n$) and rhombohedra ($R3m$) structure [51-60]. According to the research done so far, the ferromagnetism in this compound is because of the Mn^{3+} -O- Ni^{3+} super exchange interactions. In contrast, another report predicted that the main reason of ferromagnetism is Ni^{2+} -O- Mn^{4+} super exchange interactions [61-67]. Earlier report suggested that the changes in atmosphere and annealing temperature affect the magnetic properties and structure of LNMO.

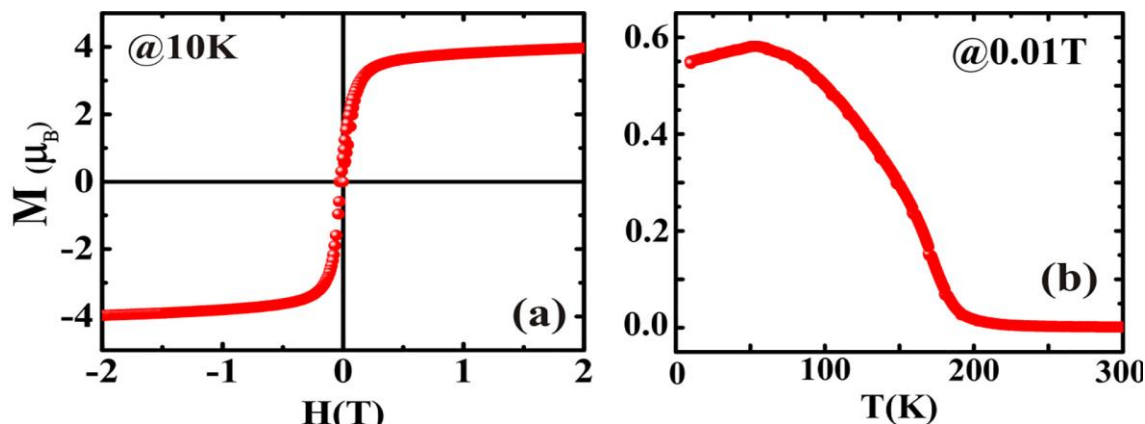
In LNMO, the anti-site cation disordering took place because of the resemblance in ionic radii of Mn and Ni cations, which makes this compound magnetically complicated [68-73]. Although synthesis of LNMO at low temperatures was a challenge, Vishwajit Gaiwad synthesized the LNMO nanoparticles via the co-precipitation method. They used two different solvents, ethanol and water [74]. Single LNMO nanoparticles were obtained at claimed temperature $600^\circ C$ using $La(NO_3)_3 \cdot 6H_2O$, $MnCl_2 \cdot 4H_2O$ and $Ni(NO_3)_2 \cdot 6H_2O$ precursors in presence of aqueous ammonia NH_4OH as precipitating agent. In order to understand the effect of solvent agent structural and magnetic properties were reported in both water and ethanol as solvent. On further calcination above $1000^\circ C$ leads to the construction of the crystalline LNMO monoclinic phase. The result obtained from powder X-ray technique shown in Figure 4, shows that the as synthesized LNMO-E is an amorphous material. Rietveld refined data obtained through XRD of LNMO-W ($600^\circ C$, 6 h) are relevant to single phase of monoclinic ($P2_1/n$) shown in Figure 4.

Figure 4. A. XRD pattern of LNMO synthesized in ethanol media; B. XRD pattern of LNMO synthesized in water media; C. XRD pattern of refinement of LNMO Nanoparticles. Note: (\bullet) Observed data; (—) Stimulated data; (—) Difference; (\uparrow) Braggs position



The magnetic characteristics of as synthesized material revealed ferromagnetic behavior whose origin is Ni²⁺-O-Mn⁴⁺ super exchange interactions. Although, only one ferromagnetic transition was observed, this suggests that the material is in single-phase as shown in Figure 5.

Figure 5. Magnetization curve at a constant temperature at 10 K and temperature varying magnetization curve.



Schematic of La₂VMnO₆

The La₂VMnO₆ (LVMO) compound in double perovskites has excellent potential because this material was theoretically predicted to be half-metallic anti-ferromagnetic. Half metallic materials were first placed in light by De Groot et al. [75-81], which showed metallic performance for one spin direction and insulating or semiconducting for another one. This type of material is applicable in spintronic devices. These materials offer a unique possibility that the state has a significant spin polarization but vanishes macroscopic magnetic moment and may be used as an exotic superconducting state, single spin superconductivity [82-85]. As reported earlier, LVMO synthesized by the art-melting method [86] shows the cubic structure with ferrimagnetism, which contrasts with earlier predicted AFM. S. Chakraverty et al. synthesized the La₂VMnO₆ thin-film by Pulsed Laser Deposition (PLD) technique on SrTiO₃ (STO) material [87,88]. XRD data reported lattice parameter of LVMO film 3.919 Å as compared to theoretically predicted lattice parameter which is 3.89 Å. The variation observed in lattice parameter was 0.75% which results due to film grown on STO [87,88]. Figure 6 shows the XRD pattern of LVMO film. LVMO film showed potential magnetic properties as shown in Figure 7.

Figure 6. XRD pattern of LVMO sample.

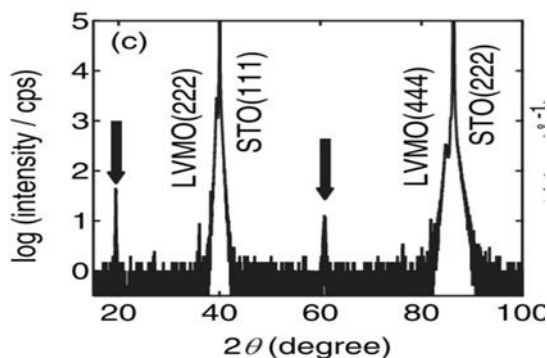
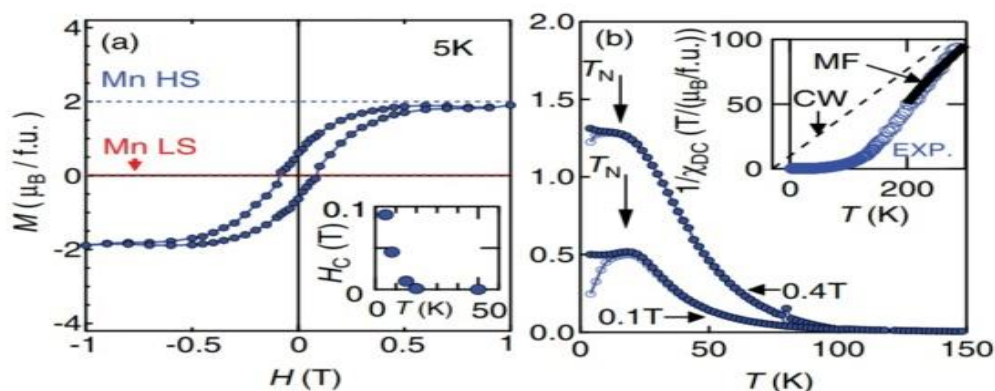


Figure 7. A. Magnetization curve at const. temperature at 5 K; B. FC and ZFC magnetization with varying temperatures.



Magnetic properties shown in **Figure 7** revealed FC and ZFC measurements. These observations propound that the temperature associated with the peak is of the order of anti-ferromagnetic temperature. Neel temperature calculated from the rise of FC and ZFC was reported at 21 K. Also reported that ground state of the material is ferromagnetic. This result is confirmed by magnetic measurements of the material with Mn^{+3} at high spin state.

Schematic of $\text{Nd}_2\text{NiMnO}_6$

Double perovskites materials have unique characteristics, i.e., double perovskite materials change their properties when rare earth elements replace A site ion with smaller ionic radii. For example, in LNMO material, La^{+3} ions are replaced by Nd^{+3} . Many properties of this material vary, and a new class of compounds is obtained. Nowadays many researchers are taking more interest in this type of material due to their various applications such as magneto electric coupling, magneto caloric effect and magneto capacitance [89]. Replacement of La^{+3} ions by Nd^{+3} ions causes the variation in Mn-O-Ni bond angles. Super exchange interaction strength is decreased through this replacement [89,90], which shows that magnetic transition temperature shrinkages monotonically as a decrement in ionic radius of ions. In $\text{Nd}_2\text{NiMnO}_6$, two types of magnetic transitions have been reported [91-94].

At high temperature, it shows ferromagnetic transition and at lower temperature magnetic anomaly. The low temperature transition was expected to be originated through $\text{Ni}^{+3}\text{-O-Mn}^{+3}$ super exchange interactions. In contrast, super exchange interactions between Mn^{+4} and Ni^{+2} get originated from high-temperature ferromagnetic transition at about 195 K. The anti-site disordered-ness in super exchange interaction between $\text{Mn}^{+4}\text{-O-Mn}^{+4}$ and $\text{Ni}^{+2}\text{-O-Ni}^{+2}$ ions results in the anti-ferromagnetism. Another possible interaction responsible for anti-ferromagnetic evolution is occurred by $\text{Ni}^{+3}(\text{Mn}^{+3})\text{-O-Ni}^{+3}(\text{Mn}^{+3})$ interaction, and ferromagnetic interaction is occurred by $\text{Ni}^{+3}\text{-O-Mn}^{+3}$ interactions [95,96]. These kinds of anti-site disordered-ness arise because of synthesis conditions like annealing temperature and time. Insufficient annealing time can disorder B and B' site ion interaction. Cederv et al. synthesized the sample $\text{Nd}_2\text{NiMnO}_6$ by solid-state reaction method using Nd_2O_3 , NiO and Mn_2O_3 as precursors. Ball milled in zirconia medium for 4 h at 295 MPa pressure, then sintered at 1223 K, 1373 K, 1523 K and 1623 K for 12 h [97,98]. XRD characterize phase identification and pureness of powder materials at 295 K. XRD pattern of

$\text{Nd}_2\text{NiMnO}_6$ is either an orthorhombic Pnma space group or a monoclinic $\text{P2}_1/\text{n}$ as shown in Figure 8. Figure 9 shows below FC and ZFC graphs, which show the ferromagnetic interaction below 200 K. Here, $\text{Mn}^{+4}\text{-O-Ni}^{+2}$ interactions are reason of ferromagnetic ordering. Low temperature behavior is the same as previously reported. Nearly at 100 K anti-site disorder took place ($\text{Ni}^{+2}\text{-O-Ni}^{+2} / \text{Mn}^{+4}\text{-O-Mn}^{+4}$ bonds) [99,100].

Figure 8. XRD pattern of $\text{Nd}_2\text{NiMnO}_6$ where A. shows $\text{P2}_1/\text{n}$. Note: (•) Y_{obs} ; (—) Y_{calc} ; (—) Y_{obs} , Y_{calc} ; (|) Bragg reflection; B. Pnma structure. Note: (•) Y_{obs} ; (—) Y_{calc} ; (—) Y_{obs} , Y_{calc} ; (|) Bragg reflection

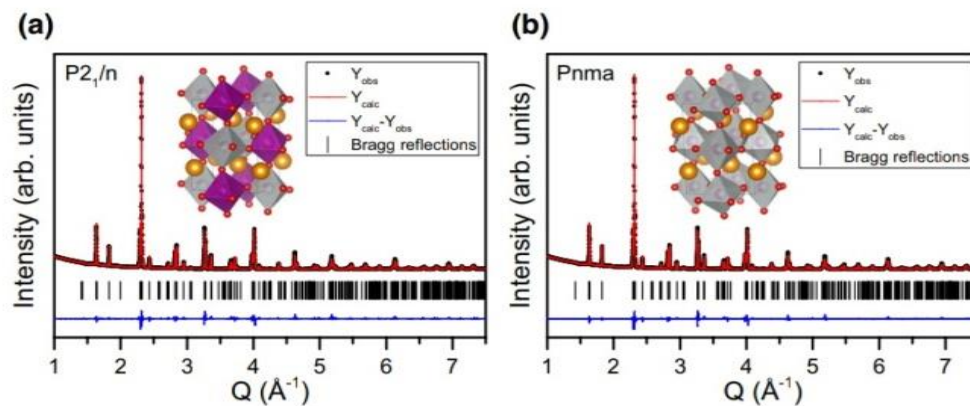
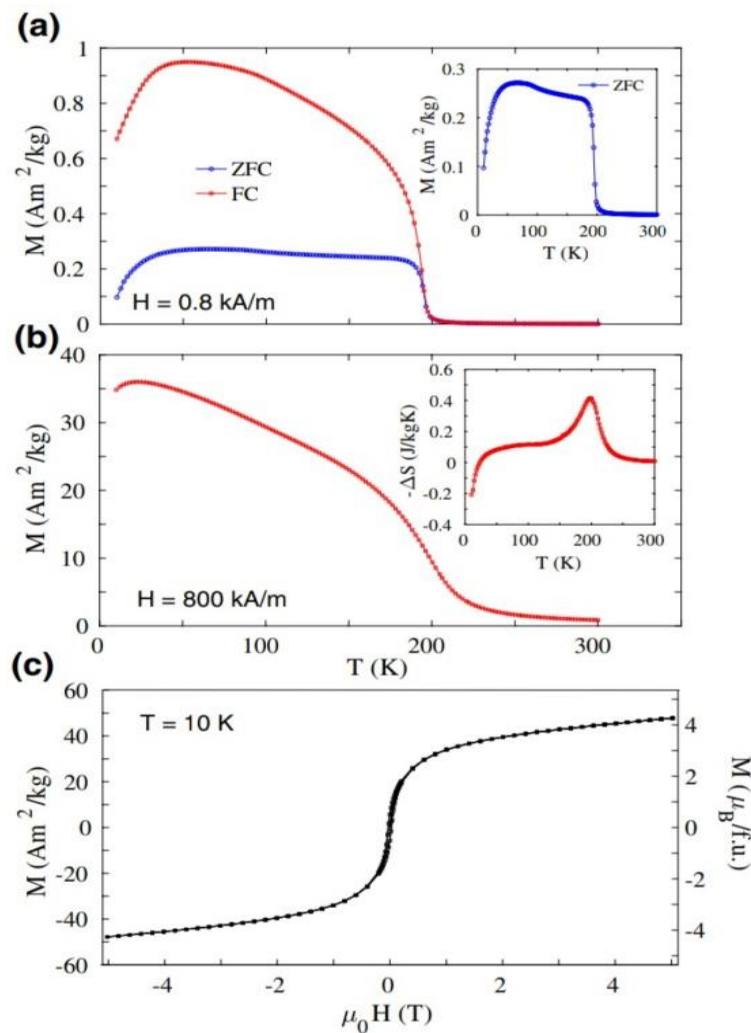


Figure 9. Curve of Magnetization versus temperature and applied magnetic field. Note: (—) ZFC; (—) FC



DISCUSSION

In addition, its sister compound $\text{La}_2\text{NiMnO}_6$ shows interesting magnetic properties and crystal structure. From the detailed study of this material we got to know that $\text{Ni}^{2+}\text{-O-Mn}^{4+}$ electronic interaction is the reason of arising enthralling magnetic properties in this material like ferromagnetism, magneto resistance, magneto capacitance etc. When $\text{La}_2\text{NiMnO}_6$ nanoparticles reported by co-precipitation method at low temperature with monoclinic phase structure. Its magnetic study shows that the nanoparticles are anti-ferromagnetic in nature. The reason of this behavior is anti-site disordered-ness between Mn-O-Mn (Ni-O-Ni) octahedral i.e., $\text{Mn}^{4+}\text{-O}^{2-}\text{-Mn}^{4+}$, $\text{Ni}^{2+}\text{-O}^{2-}\text{-Ni}^{2+}$ super exchange interaction. Another similar family material La_2VMnO_6 is a half-metallic compound. The theoretically predicted structure of La_2VMnO_6 is an essential perovskite unit cell of substance. When La_2VMnO_6 deposited on STO film, its lattice parameter increases, more significant by 0.75%, and magnetic properties are anti-ferromagnetism and ordering of spin magnetic moment acquired with Mn^{3+} at high spin state. In order to understand the changes in parental properties of double perovskite, a site cation was replaced by Nd and studied thoroughly by researchers. $\text{Nd}_2\text{NiMnO}_6$ synthesized through solid-state reaction method reported monoclinic $\text{P2}_1/\text{n}$ crystal structure and the magnetic system is ferromagnetic at high temperature and antiferromagnetic at low temperature.

Reported structure and magnetic behavior of all the above reviewed materials with different synthesis methods is concluded in [Table 1](#).

Table 1. Reported structure and magnetic behavior of A_2XYO_6 with different synthesis methods.

Material	Synthesis Method	Structure	Magnetic	Refer ence
$\text{La}_2\text{CrMnO}_6$	Ceramic Technique	<ul style="list-style-type: none"> Monoclinic 	<ul style="list-style-type: none"> Ferromagnetic 	[38]
	Combustion Method	<ul style="list-style-type: none"> Rhombohedral 	<ul style="list-style-type: none"> Ferromagnetic Double exchange interaction 	[35]
	Combustion Method	<ul style="list-style-type: none"> Orthorhombic 	<ul style="list-style-type: none"> Multiple Magnetic Transition: ferromagnetic, spinglass, and Griffith-like phases 	[36]
	Solid state reaction	<ul style="list-style-type: none"> Orthorhombic 	<ul style="list-style-type: none"> Ferromagnetic or ferrimagnetic Double exchange interaction 	[42]
	Solid state reaction	<ul style="list-style-type: none"> Orthorhombically distorted perovskite structure 	<ul style="list-style-type: none"> Ferromagnetic and antiferromagnetic Super exchange interaction 	[39]
	Glycine nitrate	<ul style="list-style-type: none"> As prepared Orthorhombic Anneal at 1300°C 	<ul style="list-style-type: none"> antiferromagnetic antisite 	[57]

La₂NiMnO₆		→ Rhombohedral	<ul style="list-style-type: none"> Disorder 	
	Pechini Method	<ul style="list-style-type: none"> As prepared Rhombohedral Anneal at T >800°C → Monoclinic and Rhombohedral 		[55]
	Ethylene glycol gel method	<ul style="list-style-type: none"> Coexistence of Rhombohedral and Orthorhombic 		[60]
	PVA sol gel method	<ul style="list-style-type: none"> Rhombohedral 		[64]
La₂VMnO₆	Theoretical Method (Generalized gradient approximation)	<ul style="list-style-type: none"> Cubic and Tetragonal 	<ul style="list-style-type: none"> FM and AFM 	[88]
	Art melting	<ul style="list-style-type: none"> Cubic 	<ul style="list-style-type: none"> FM 	[86]
	Pulsed laser deposition	<ul style="list-style-type: none"> Cubic 	<ul style="list-style-type: none"> FM 	[77]
Nd₂NiMnO₆	Solid-state reaction method	<ul style="list-style-type: none"> Orthorhombic Pnma space group or a monoclinic P2₁/n 	<ul style="list-style-type: none"> ferromagnetic transition high-temperature Ni⁺³-O-Mn⁺³ interactions anti-ferromagnetism low-temperature Ni⁺³(Mn⁺³)-O-Ni⁺³(Mn⁺³) interaction 	[96]

CONCLUSION

In this review, we briefly reviewed the current research on double perovskite materials covering mainly structural and magnetic properties. B-site cation largely affects the properties of double perovskite materials. As we have discussed that the substitution at A and B site ions affects the magnetic and structural characteristics. It was also reviewed that different synthesis methods affect magnetic and structural characteristics of double perovskites because change in synthesis method changes the type of exchange interaction. Magnetic nature of pulse laser deposited La₂CrMnO₆ material suggests that the ground state of La₂CrMnO₆ is ferrimagnetic. Whereas La₂CrMnO₆ synthesized by solid-state reaction method, an orthorhombic Pbnm crystal structure is acquired as soft magnetic substance with a minor coercive field. Magnetic behaviour is attributable to Cr⁺³-O²⁻-Mn⁺³ exchange interaction. La₂CrMnO₆ prepared by sol gel acquires orthorhombic structure with the Pbnm group.

REFERENCES

1. Ji F, et al. The atomic-level structure of bandgap engineered double perovskite alloys. Chem Sci. 2021; 12:1730.

2. Tao Q, et al. Machine learning for perovskite materials design and discovery. *npj Computational Materials*. 2021; 7:23.
3. Sarma DD, et al. A new class of magnetic materials: $\text{Sr}_2\text{FeMoO}_6$ and related compounds. *Curr Opin Solid State Mater Sci*. 2001; 5:261-268.
4. Vasala S, et al. $\text{A}_2\text{B}'\text{B}''\text{O}_6$ perovskites: A review. *Prog Solid State Chem*. 2015; 1:43.
5. Bhalla AS, et al. The perovskite structure-a review of its role in ceramic science and technology. *Mater Res Innov*. 2000; 4:3-26.
6. Anderson MT, et al. B-cation arrangements in double perovskites *Prog. Solid State Chem*. 1993; 22:197-233.
7. Nissar U, et al. Impact of A-site rare earth substitution on structural, magnetic, optical and transport properties of double perovskites. *Materials Research Bulletin*. 2020; 127:110844.
8. Chmaissem O, et al. Structural phase transition and the electronic and magnetic properties of $\text{Sr}_2\text{FeMoO}_6$. *Phys Rev B*. 2000; 62:14197. [Crossref] [Google Scholar]
9. Gupta A, et al. Grain-boundary effects on the magnetoresistance properties of perovskite manganite films. *Phys Rev B*. 1996; 54:15629.
10. T. Sugahara, et al. Structural and semiconductor-to-metal transitions of double perovskite cobalt oxide $\text{Sr}_{2-x}\text{La}_x\text{CoTiO}_{6-\delta}$ with enhanced thermoelectric capability. *Appl Phys Lett*. 2011; 99:62103.
11. Viswanathan M, et al. Influence of lattice distortion on the Curie temperature and spin-phonon coupling in $\text{LaMn}_{0.5}\text{Co}_{0.5}\text{O}_3$. *J Phys Condens Matter*. 2010; 22:346006.
12. Mahato RN, et al. Colossal magnetoresistance in double perovskite oxide $\text{La}_2\text{CoMnO}_6$. *J Appl Phys*. 2010; 107:09D714.
13. Blackstead HA, et al. Comment on "Origin of the superconductivity in the Y-Sr-Ru-O and Y-Sr-Cu-O systems. *Phys Rev B*. 2009; 79:16501.
14. Eng HW, et al. Investigations of the electronic structure of d0 transition metal oxides belonging to the perovskite family. *J Solid State Chem*. 2003; 175:94.
15. Dandia A, et al. Visible light driven perovskite-based photocatalysts: A new candidate for green organic synthesis by photochemical protocol. *Curr Opin Green Sustain*. 2020; 3:100031.
16. Battle PD, et al. The crystal structures and magnetic properties of $\text{Ba}_2\text{LaRuO}_6$ and $\text{Ca}_2\text{LaRuO}_6$. *J Solid State Chem*. 1983; 46:234.
17. Schinzer C, et al. A new ferromagnetic perovskite: $\text{LaMn}_{1/2}\text{Rh}_{1/2}\text{O}_3$. *J Phys Chem Solids*. 2000; 61:01543-1551.

18. Greedan JE, et al. A search for disorder in the spin glass double perovskites $\text{Sr}_2\text{CaReO}_6$ and $\text{Sr}_2\text{MgReO}_6$ using neutron diffraction and neutron pair distribution function analysis. *J Phys Condens Matter*. 2011; 23: 164213.
19. Pinacca RM, et al. Preparation, crystal structure and magnetic behavior of new double perovskites $\text{Sr}_2\text{B}'\text{UO}_6$ with $\text{B}'=\text{Mn, Fe, Ni, Zn}$. *J Solid State Chem*. 2007; 180:1582.
20. Battle PD, et al. The crystal and magnetic structures of $\text{Sr}_2\text{LuRuO}_6$, Ba_2YRuO_6 , and $\text{Ba}_2\text{LuRuO}_6$. *J Solid State Chem*. 1989; 78:108.
21. Baron-Gonzalez AJ, et al. Effect of cation disorder on structural, magnetic and dielectric properties of $\text{La}_2\text{MnCoO}_6$ double perovskite. *J Phys Condens Matter*. 2011; 23:496003.
22. Asai K, et al. Magnetization Measurements and ^{55}Mn NMR Studies of $\text{LaNi}_{0.5}\text{Mn}_{0.5}\text{O}_3$. *J Phys Soc Jpn*. 1979; 47:1054.
23. Sanchez-Benitez J, et al. Magnetic and structural features of the $\text{NdNi}_{1-x}\text{Mn}_x\text{O}_3$ perovskite series investigated by neutron diffraction. *J Phys Condens Matter*. 2011; 23:226001.
24. Palkar VR, et al. Observation of magnetoelectric behavior at room temperature in $\text{Pb}(\text{Fe}_x\text{Ti}_{1-x})\text{O}_3$. *Solid State Commun*. 2005; 134:783-786.
25. Vasala S, et al. Degree of order and redox balance in B-site ordered double-perovskite oxides, $\text{Sr}_2\text{MMoO}_{6-\delta}$ ($\text{M}=\text{Mg, Mn, Fe, Co, Ni, Zn}$). *J Solid State Chem*. 2010; 183:1007-1012.
26. Chu L, et al. Lead-Free Halide Double Perovskite Materials: A New Superstar toward Green and Stable Optoelectronic Applications. *Nano-Micro Letters*. 2019; 11:244-246.
27. Kobayashi KI, et al. Room-temperature magnetoresistance in an oxide material with an ordered double-perovskite structure. *Nature*. 1998; 395:677-680.
28. Saha-Dasgupta T, et al. Double perovskites with 3d and 4d/5d transition metals: compounds with promises. *Mater Res Express*. 2020; 7:014003.
29. Teresa JMD, et al. Impact of cation size on magnetic properties of $(\text{AA}')_2\text{FeReO}_6$ double perovskites. *Phys Rev B*. 2004; 69:144401.
30. Kato H, et al. Structural and electronic properties of the ordered double perovskites A_2MReO_6 ($\text{A} = \text{Sr, Ca}$; $\text{M} = \text{Mg, Sc, Cr, Mn, Fe, Co, Ni, Zn}$). *Phys Rev B*. 2004; 69:184412.
31. Sikora M, et al. Evidence of unquenched Re orbital magnetic moment in $\text{AA}'\text{FeReO}_6$ double perovskites. *Appl Phys Lett*. 2006; 89:062509.
32. Serrate D. et al. Double perovskites with ferromagnetism above room temperature. *J Phys Condens Matter*. 2007; 19:023201.
33. Fisher B, et al. Variable range hopping in A_2MnReO_6 ($\text{A}=\text{Ca, Sr, Ba}$). *J Appl Phys*. 2008; 16:104.
34. Rogado NS, et al. Magnetocapacitance and magnetoresistance near room temperature in a ferromagnetic semiconductor: $\text{La}_2\text{NiMnO}_6$. *Adv Mater*. 2005; 17:2225.
35. Barrozo P, et al. Ferromagnetism in Mn half-doped LaCrO_3 perovskite. *J Appl Phys*. 2013; 113: 17E309.
36. Palakkal JP, et al. Multiple magnetic transitions, Griffiths-like phase, and magnetoresistance in $\text{La}_2\text{CrMnO}_6$. *J Appl Phys*. 2017; 122:073907.
37. Singh D, et al. Effect of A-site cation size on the structural, magnetic, and electrical properties of $\text{La}_{1-x}\text{Nd}_x\text{Mn}_{0.5}\text{Cr}_{0.5}\text{O}_3$ perovskites. *J Alloy Compd*. 2015; 644:172–179.

38. Bents UH, et al. Neutron diffraction study of the magnetic structures for the perovskite type mixed oxides La (Cr, Mn) O₃. *Phys Rev.* 1957; 106:225–230.
39. Karpinsky DH, et al. Inhomogeneous magnetic states in Fe and Cr substituted LaMnO₃. *J Phys Condens Matter.* 2007; 19:036220.
40. Yoshimatsu K, et al. Magnetic and electronic properties of B-site-ordered double-perovskite oxide La₂CrMnO₆ thin films. *Phys.Rev B.* 2019; 99:235129.
41. Yang Z, et al. Density-functional studies of magnetic and electronic structures for the perovskite oxides LaMn_{1-x}Cr_xO₃. *J Phys Condens Matter.* 2000; 12:2737.
42. Sun Y, et al. Possible double-exchange interaction between manganese and chromium in LaMn_{1-x}Cr_xO₃. *Phys Rev B.* 2001; 63:174438.
43. Cohelo A, et al. A charge-flipping algorithm incorporating the tangent formula for solving difficult structures. *Coelho Software Brisbane.* 2007; 63:400-406.
44. Lima OFD, et al. Magnetic phase evolution in the LaMn_{1-x}Fe_xO_{3+y} system. *J Appl Phys.* 2009; 105(1): 013907.
45. Goodenough JB, et al. Relationship between crystal symmetry and magnetic properties of ionic compounds containing Mn³⁺. *Phys Rev.* 1961; 124:373–384.
46. Yang D, et al. Ferrimagnetism, resistivity, and magnetic exchange interactions in double perovskite La₂CrMnO₆. *Results in Physics.* 2019; 12: 344–348.
47. Goodenough JB, et al. Theory of the Role of Covalence in the Perovskite-Type Manganites [La, Mn(II)]MnO₃. *Phys Rev.* 1955; 100:564.
48. Kanamori J, et al. Superexchange interaction and symmetry properties of electron orbitals. *J Phys Chem Solids.* 1959; 10:87-98.
49. Tirmali PM, et al. Effects of partial site substitution on magnetic and dielectric behavior of La₂NiMnO₆ double perovskite. *J Mater Sci Mater Electron.* 2016; 27:4314-4320.
50. Choudhury D, et al. Near-room-temperature colossal magnetodielectricity and multiglass properties in partially disordered La₂NiMnO₆. *Phyas Rev Lett.* 2012; 108:127201.
51. Ravi S, et al. Room temperature ferromagnetism with high Curie temperature in La₂MnNiO₆ nanoparticle. *Mater Lett.* 2016; 164: 124–126.
52. Chen H, et al. The giant dielectric constant and tunable properties of La₂NiMnO_{6-x}MgO ceramics. *J Alloys Compd.* 2014; 616: 213–220.
53. Sayed FN, et al. Role of annealing conditions on the ferromagnetic and relaxor properties of La₂NiMnO₆. *J Mater Res.* 2011; 4: 567.
54. Barbosa DAB, et al. Ba-doping effects on structural, magnetic and vibrational properties of disordered La₂NiMnO₆. *J Alloys Compd.* 2016; 663: 899–905.
55. Dass RI, et al. Oxygen stoichiometry, ferromagnetism, and transport properties of La_{2-x}NiMnO_{6+δ}. *Phys Rev B.* 2003; 68: 64415.
56. Anderson MT, et al. B-cation arrangements in double perovskites. *Prog Solid State Chem.* 1993; 22:197-233.
57. Joseph VLJ, et al. Two ferromagnetic phases with different spin states of Mn and Ni in LaMn_{0.5}Ni_{0.5}O₃. *Phys Rev B.* 2002; 65: 184416.

58. Bull CL, et al. Determination of B-site ordering and structural transformations in the mixed transition metal perovskites $\text{La}_2\text{CoMnO}_6$ and $\text{La}_2\text{NiMnO}_6$. *J Phys Condens Matter*. 2003; 15:4927.
59. Cao Z, et al. The electric and dielectric responses of $\text{La}_2\text{Ni}_{1-x}\text{Mg}_x\text{MnO}_6$ solid solution. *J Alloys Compd*. 2015; 628: 81–88.
60. Chandrasekhar KD, et al. Synthesis and Magnetic Properties Of $\text{La}_2\text{NiMnO}_6$ Nanoparticles, *AIP Conf Proc*. (n.d.) 2012; 23: 1347.
61. Wang X, et al. The influence of the anti-ferromagnetic boundary on the magnetic property of $\text{La}_2\text{NiMnO}_6$. *Appl Phys Lett*. 2009; 95: 252502.
62. Mao YB, et al. Magnetic properties of double perovskite La_2BMnO_6 (B = Ni or Co) nanoparticles. *Nanoscale*. 2013; 5: 4720–4728.
63. Leng K, et al. Recent advances in Re-based double perovskites: Synthesis, structural characterization, physical properties, advanced applications, and theoretical studies. *AIP Advances*. 2020; 10: 120701.
64. Li C, et al. Preparation, characterization and dielectric tunability of $\text{La}_2\text{NiMnO}_6$ ceramics. *J. Alloys Compd*. 2014; 590: 541–545.
65. Cao Z, et al. Extrinsic and intrinsic contributions for dielectric behavior of $\text{La}_2\text{NiMnO}_6$ ceramic. *Phys B Condens Matter*. 2015; 477: 8–13.
66. Kumar P, et al. Temperature dependent magnetic, dielectric and Raman studies of partially disordered $\text{La}_2\text{NiMnO}_6$. *Solid State Commun*. 2014; 184: 47–51.
67. Hashisaka M, et al. Spin-filtering effect of ferromagnetic semiconductor $\text{La}_2\text{NiMnO}_6$. *J Magn Magn Mater*. 2007; 310: 1975–1977.
68. Murthy JK, et al. Observation of Griffiths-like phase and its tunability in $\text{La}_2\text{Ni}_{1-x}\text{Co}_x\text{MnO}_6$ ($0 < x < 1$) nanoparticles. *J Magn Mater*. 2016; 2–8.
69. Lan C, et al. Investigation on structures, band gaps, and electronic structures of lead free $\text{La}_2\text{NiMnO}_6$ double perovskite materials for potential application of solar cell. *J Alloys Compd*. 2016; 655: 208–214.
70. Zhao S, et al. Size-dependent magnetic properties and Raman spectra of $\text{La}_2\text{NiMnO}_6$ nanoparticles. *J Appl Phys*. 2009; 106: 123901.
71. Luo X, et al. The magnetic entropy change in the double perovskite $\text{La}_2\text{NiMnO}_6$ with strong spin – phonon coupling. *Solid State Commun*. 2009; 149: 810–813.
72. Wu Z, et al. Double-perovskite magnetic $\text{La}_2\text{NiMnO}_6$ nanoparticles for adsorption of bovine serum albumin applications. *Nanoscale Res Lett*. 2013; 8: 207.
73. Zhang Z, et al. Synthesis and characterization of ordered and disordered polycrystalline $\text{La}_2\text{NiMnO}_6$ thin films by sol–gel. *Dalt Trans*. 2012; 41: 11836.
74. Gaikwada VM, et al. New low temperature process for stabilization of nanostructured $\text{La}_2\text{NiMnO}_6$ and their magnetic properties. *J Magn Magn Mater*. 2019; 471: 8-13.
75. Zu N, et al. Pressure-Induced Half-Metallic Ferrimagnetism in La_2VMnO_6 . *J Phys Chem C*. 2013; 117: 7231-7235.
76. Groot D, et al. New Class of Materials: Half-Metallic Ferromagnets. *J Phys Rev Lett*. 1983; 50: 2024-2027.

77. Chakraverty S, et al. Magnetic and Electronic Properties of Ordered Double-Perovskite. *Phys Rev B*. 2011; 84: 132411.
78. Leuken HV, et al. Half-Metallic Antiferromagnets. *Phys Rev Lett*. 1995; 74: 1171.
79. Rudd RE, et al. Single-spin superconductivity: Formulation and Ginzburg-Landau theory. *Phys Rev B*. 1998; 57: 557.
80. Luo H, et al. Ab initio study of Cr substitution for Co in the Heusler alloy Co_2CrAl : Half-metallicity and adjustable magnetic moments. *Phys B*. 2008; 403: 1797.
81. Lee JI, et al. Predicted half-metallicity with no net magnetization in $\text{Ca}_{0.75}\text{Cr}_{0.25}\text{As}$ from a first-principles study. *J Appl Phys*. 2009; 105: 07E508.
82. Long NH, et al. New type of half-metallic antiferromagnet: transition metal pnictides. *J. Phys. Condens. Matter*. 2009; 21: 064241.
83. Pickett WE. Spin-density-functional-based search for half-metallic antiferromagnets. *Phys. Rev. B*. 1998; 57, 10613.
84. Lee KW and Pickett WE. Half semimetallic antiferromagnetism in the Sr_2CrTO_6 system (T=Os,Ru). *Phys. Rev. B*. 2008; 77: 115101.
85. Park JH, et al. Half-metallic antiferromagnetic double perovskites: LaAVRuO_6 (A=Ca, Sr, and Ba). *Phys. Rev. B*. 2002; 65: 174401.
86. Androulakis J, et al. Realization of La_2VMnO_6 : Search for Half-Metallic Anti-ferromagnetism. *Solid State Commun*. 2002; 124: 77–81.
87. Wang YK, et al. Robust half-metallic antiferromagnets LaAVOsO_6 and LaAMoYO_6 (A=Ca,Sr,Ba; Y=Re,Tc) from first-principles calculations. *Phys Rev B*. 2006; 73: 064424.
88. Chen SH, et al. Stability of Half-Metallic Antiferromagnet La_2VMnO_6 , First-principles Calculation Study. *Physica B*. 2011; 406: 2783–2787.
89. Nasir M, et al. Role of Antisite Disorder, Rare-Earth Size, and Superexchange Angle on Band Gap, Curie temperature, and Magnetization of R_2NiMnO_6 Double Perovskites. *ACS Appl Electr Mater*. 2019; 1: 141.
90. Faske T, et al. X-ray diffractometer for the investigation of temperature- and magnetic field-induced structural phase transitions. *J Appl Crystallogr*. 2018; 51: 761.
91. Shi C, et al. Local valence and physical properties of double perovskite $\text{Nd}_2\text{NiMnO}_6$. *J Phys D*. 2011; 44: 245405.
92. Yadav R, et al. Magnetic frustration and dielectric relaxation in insulating $\text{Nd}_2\text{NiMnO}_6$ double perovskites. *J Appl Phys*. 2015; 117: 053902.

93. Ali A, et al. Rare-earth tuned magnetism and magnetocaloric effects in double perovskites R_2NiMnO_6 . Journal of Physics: Condensed Matter. 2021; 34: 9.
94. Moon JY, et al. Giant Anisotropic Magnetocaloric Effect in Double-perovskite Gd_2CoMnO_6 Single Crystals. Sci. Rep. 2017; 7: 16099.
95. Pal S, et al. Peculiar magnetic states in the double perovskite Nd_2NiMnO_6 . Phys Rev B. 2019; 100: 045122.
96. Cedervall J, et al. On the structural and magnetic properties of the double perovskite Nd_2NiMnO_6 . J Mater Sci Mater Electron. 2019; 21: 751.
97. Baltrus JP, et al. Rare earth oxides Eu_2O_3 and Nd_2O_3 analyzed by XPS. Surf Sci Spectra. 2019; 26: 014001.
98. Blascoa J, et al. Synthesis and structural study of $LaNi_{1-x}Mn_xO_{3+\delta}$ perovskites. J Phys Chem Solids. 2002; 63:781.
99. Singh G, et al. Effect of oxygen pressure on structural and magnetic properties of Nd_2NiMnO_6 thin films grown on different substrates. J Alloys Compd. 2018; 739: 586-589.
100. Khan JA, et al. Double perovskite La_2CrMnO_6 : synthesis, optical and transport properties. Mater Res Express. 2019; 6: 115906.